

## **Fabrication of Electrochemical Sensor for Hyaluronic Acid Determination**

*Chen Chen, Junfang Li, Xiaoli Bai, Ke Pei, Mingyue Wang, Hongqiao Zhao, Linlin Yang and Caie Wang\**

Department of Clinical Pharmacy, the First Affiliated Hospital of Henan University of Science and Technology P.R. China

\*E-mail: [wangcaie890@sohu.com](mailto:wangcaie890@sohu.com)

*Received: 15 April 2017 / Accepted: 2 June 2017 / Published: 12 July 2017*

---

This work employed a facile one-pot hydrothermal method to prepare a reduced graphene oxide-ZnO nanorods composite (RGO-ZnO). Glassy carbon electrode (GCE) was modified by the obtained nanocomposite, which was then used to realize the selective and sensitive detection of hyaluronan (HY). The fabricated biosensor was linearly related to HY concentration (1 - 800  $\mu\text{M}$ ), with a limit of detection (LOD) of 0.42  $\mu\text{M}$  (S/N = 3). This biosensor for HY was stable, reproducible and characteristic of anti-interference. Furthermore, the proposed biosensor has potential for further application in HY detection in gecko extract specimens.

---

**Keywords:** Electrochemical sensor; Graphene; Zinc oxide; Hyaluronan; Gecko extract

### **1. INTRODUCTION**

Hyaluronate (HY), also termed hyaluronic acid and hyaluronan, is an extracellular polysaccharide that was originally characterized in the vitreous humor [1]. HY and other glycosaminoglycans comprise a typical class of compounds in the connective tissues of vertebrates [2]. The barrier against the spread of infectious agents and macromolecules, regulation of plasma protein distribution, water homeostasis, joint lubrication, extracellular matrix stabilization, and cellular activities regulation via interactions with receptor proteins on the cell surface and other functions have been attributed to HY [3]. Moreover, HY is significantly correlated with several well-known pathological cases in which HA in the serum increases, particularly in joint and liver diseases but also in cancer, uremia, septicemia, Hutchinson–Gilford progeria syndrome, Werner’s syndrome, myelofibrosis, systemic sclerosis, etc [4]. The survival of cancer cells depends on their capacity for

adhering to the tissue matrix, proliferating, migrating and invading the tissue, and traveling and settling as metastases without being destroyed by immune reactivity.

Previously, HY has been quantitatively analyzed by separating it from other polysaccharides via various approaches, and by colorimetric analyses such as uronic acid detection using the carbazole technique [5-8]. The finding of the specific binding between HY and the proteins in cartilage resulted in the proposal of a novel theory for the specific determination of HY [9-12]. Then, Tengblad [12] reported a radiometric analysis based on the competition of free HY in solution and HY-substituted Sepharose gel with HY-binding cartilage protein (HABP) labeled with  $^{125}\text{I}$ . Through modification, this analytical method can not only determine HA in biological specimens [13-15] but also measure HY (nanogram) and is 100-fold more sensitive than the previous methods. Thereafter, different modified techniques were proposed, such as a competitive enzyme-linked immunosorbent assay (ELISA) [16-18], a competitive fluorescence-based assay [19], and noncompetitive ELISA-like assays [20, 21], where the principle of the affinity of certain extracellular matrix to HY are the same. Unfortunately, many of these techniques have disadvantages. For instance, the enzymatic technique is not only costly but also easy to produce metabolites.

The simple, rapid, and sensitive electrochemical technique is regarded as a more proper method for biomolecule detection. Nevertheless, this method also has several drawbacks such as poor reproducibility and stability. Carbon materials have gained widespread application in electrocatalysis and electroanalysis. For instance, carbon nanotubes exhibit desirable behavior in biofuel cells and biosensors. In contrast, graphene is potentially safe, possesses a high surface area, and can be easily processed. Compared with the commercial GCE, graphene exhibits a higher apparent electron-exchange rate constant, 0.49 cm/s [22-28]. Furthermore, the 2D structure of graphene is favorable for the fabrication of electrochemical sensors for specific target determination. In electrochemistry, zinc oxide is among the more extensively studied transition metal oxides. As indicated in several studies, ZnO nanoparticles are promoted by its electrocatalytic activity when they are used to modify graphene sheets. Nayak and co-workers [29] reported a ZnO/graphene nanocomposite-based electrochemical dopamine sensor with desirable behavior. Jiang and co-workers [30] proposed a graphene-ZnO nanocomposite to electrochemically and ultrasensitively sense phenacetin and acetaminophen.

In this work, an electrochemical biosensor for HY detection was constructed using the reduced graphene oxide-ZnO nanorods (RGO-ZnO) composite synthesized by means of a facile one-pot technique. X-ray diffraction (XRD) and Raman spectroscopy were employed to characterize the obtained nanocomposite. HY detection was realized based on the proposed biosensor via cyclic voltammetry (CV) and potentiostatic techniques. The fabricated biosensor was further utilized for HY detection in real gecko extract specimens.

## 2. EXPERIMENTS

### 2.1. Materials

Graphene oxide powder was purchased from JCNANO, INC. Hyaluronan (HY), hydrazine solution (25% in water) and zinc nitrate hexahydrate ( $\text{Zn}(\text{NO}_3)_2 \cdot 6\text{H}_2\text{O}$ ) were purchased from Sigma-

Aldrich. All other reagents were of analytical grade, without being further purified.  $K_2HPO_4$  and  $KH_2PO_4$  solution (0.1 M) were mixed together to a proper pH value to obtain phosphate buffer solution (PBS). Milli-Q water of 18.2 M $\Omega$  cm was employed in all tests.

## 2.2. Preparation of RGO-ZnO nanocomposite

The preparation of RGO-ZnO is described as follows. A 10 mL aliquot of water was mixed with GO (10 mg) under 2 h sonication to obtain a 1 mg/mL GO dispersion. Subsequently, the GO dispersion was gradually added with  $Zn(NO_3)_2 \cdot 6H_2O$  (10 mL, 50 mM) under stirring. Then, hydrazine solution (2 mL, 5 wt%) was sonicated for 60 min and added to the above mixture to obtain a gray slurry. After being stirred for 60 min, the slurry was introduced to a Teflon-lined stainless steel autoclave (30 mL), and heated for 120 min at 120°C. Following centrifugation, the as-prepared slurry was dried in an oven at 70°C to obtain RGO-ZnO nanocomposite.

## 2.3. Gecko sample preparation

After pulverization, 1 g of dry gecko powder was refluxed using 50 mL of aqueous ethanol (70%) for 60 min at 80°C. After cooling, the reflux was filtrated using a paper filter to obtain a mixture of washings and extract, which was concentrated to ca. 40 mL in a vacuum. After dilution, the obtained solution (50 mL) was used as the real specimen.

## 2.4. Characterizations and measurement

An XRD with Cu K $\alpha$  radiation (D8-Advanced, Bruker, Germany) was employed to obtain X-ray diffraction profiles (5° - 90° in 2 $\theta$ ). A Raman Microprobe (Renishaw RM1000) with laser light (514 nm) was used to perform Raman spectroscopy at ambient temperature. After polishing with alumina-water slurry, GCE was rinsed with water before electrochemical analysis. This was followed by dropping catalyst dispersion (7  $\mu$ L, 0.5 mg/mL) onto the surface of the as-prepared GCE, which was then left to dry at ambient temperature. The prepared electrodes were denoted as ZnO/GCE, RGO/GCE and RGO-ZnO/GCE. A CH Instruments 660A electrochemical Workstation (CHI-660 A, CH Instruments, Texas, USA) with a triple-electrode configuration was applied for electrochemical assays. Herein the reference and auxiliary electrode were Ag/AgCl (3M KCl) and a platinum wire, respectively. Cyclic voltammetry was conducted in 10.0 mL of 0.1 M PBS at a scan rate of 50 mV/s. The amperometric response was collected at a fixed potential of 0.37 V.

## 3. RESULTS AND DISCUSSION

GO reduction under hydrothermal circumstance was confirmed using Raman spectroscopy with significant sensitivity to the electronic structure of carbon based materials. Two characteristic peaks

for both RGO-ZnO nanocomposite and GO appear at  $1340$  and  $1578\text{ cm}^{-1}$ , corresponding to the diamondoid (D) and graphite (G) bands (Fig. 1A). There is an increase in the intensity ratio of D/G from  $0.92$  to  $1.13$  after hydrothermal treatment, which suggests that the reduction process has occurred, followed by an increase in the concentration of defect in RGO sheets [31]. GO and RGO-ZnO nanocomposite were characterized via XRD profiles, as indicated in Fig. 1B. A significant peak can be observed for GO at  $11.2^\circ$ , representing the (001) lattice plane, which was confirmed previously [32]. RGO-ZnO nanocomposite was characterized via a diffractogram, in which peaks appear at  $31.4$ ,  $34.2$ ,  $35.7$ ,  $47.4$ ,  $56.2$ ,  $62.5$  and  $67.4^\circ$ . These findings indicate that the ZnO nanoparticles decorated on the graphene sheets are of the hexagonal wurtzite phase with a size of  $12\text{--}23\text{ nm}$  according to the Scherer formula [33]. Furthermore, GO reduction during hydrothermal treatment is also demonstrated by the presence of a novel wide peak centered at  $26.4^\circ$  (002) and the disappearance of the diffraction peak of GO at  $11.2^\circ$ . It has been reported that, if the regular stacks of GO or graphite are destroyed, for example by exfoliation, their diffraction peaks become weak or may even disappear [34].

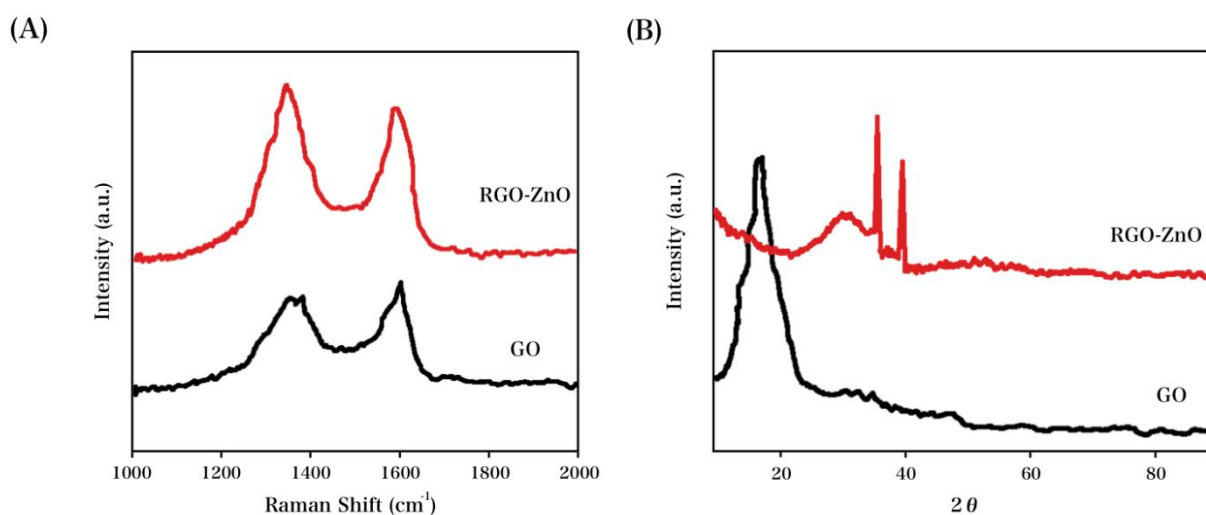


**Figure 1.** (A) Raman spectra of the nanocomposite of GO and RGO-ZnO. (B) XRD profiles of the nanocomposite of GO and RGO-ZnO.

The analysis of the electrochemical performance of  $0.5\text{ mM}$  HY was separately realized through cyclic voltammetry. As indicated in Fig. 2, the electrochemical performance of HY ( $0.5\text{ mM}$ ) at the GCE, ZnO/GCE, RGO/GCE, and RGO-ZnO/GCE was characterized via CVs. Without the addition of HY, the RGO-ZnO modified GCE exhibits no pronounced peaks (Fig. 2). In contrast, the GCE, ZnO/GCE, RGO/GCE, and RGO-ZnO/GCE exhibit obvious peaks for HY, where the current response is respectively  $0.0173$ ,  $0.0323$ ,  $0.0668$  and  $0.1169\text{ mA}$ . Furthermore, the oxidation potential of HY at the original GCE, ZnO, RGO and RGO-ZnO modified GCE is respectively  $0.48$ ,  $0.43$ ,  $0.42$  and  $0.37\text{ V}$ . In comparison with the original GCE, ZnO/GCE, RGO/GCE, and RGO-ZnO/GCE exhibit desirable electrocatalytic activity for HY determination, as indicated by the peak potential decrease and peak current increase. The enhancement probably resulted from the large surface-to-volume ratio,

high electrical conductivity, favorable biocompatible, excellent catalytic ability and surface reaction activity.

The influence of the scan rate on the electrocatalytic oxidation of HY at RGO-ZnO/GCE was investigated in this work. The RGO-ZnO modified GCE with the addition of HY (0.5 mM) was characterized via CVs (20 - 260 mV/min). Along with the rise of the scan rate, there is an increase in the peak current, with a shift of the oxidization potential in the positive direction (Fig. 3A). This is possibly due to the kinetic limitation of the reaction between the redox sites of the RGO-ZnO and HY, in agreement with previous works [35, 36].

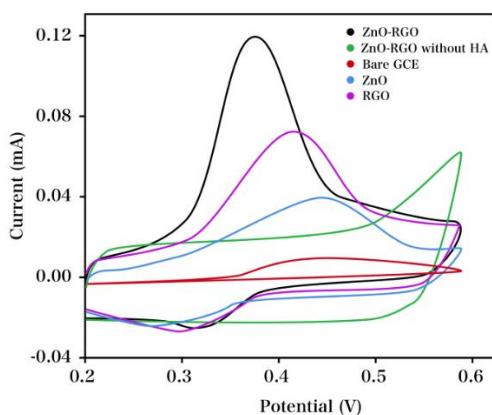


**Figure 2.** CVs of the original, ZnO/GCE, RGO/GCE and RGO-ZnO/GCE in PBS (0.1 M) with or without HY (0.5 mM). Scan rate: 50 mV/s.

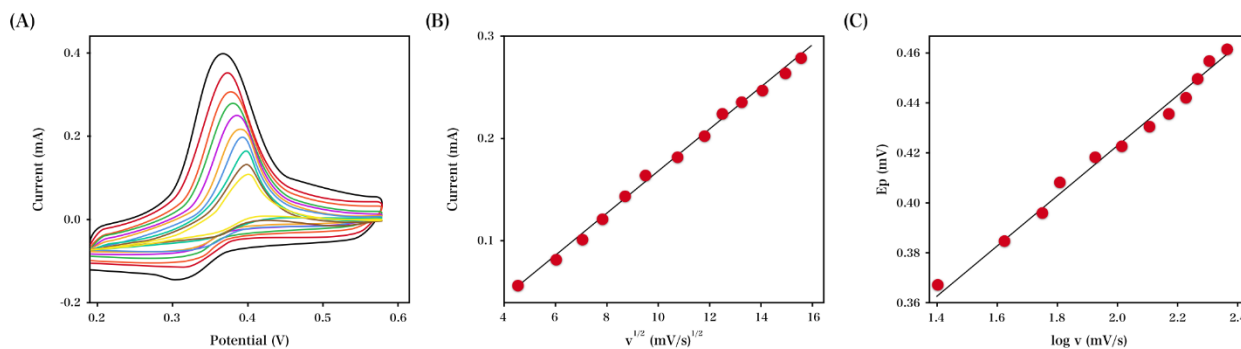


**Figure 3.** (A) CVs of the RGO-ZnO/GCE in PBS (0.1 M) containing HY (1 mM) at a scan rate of 20—260 mV/s. (B) Plots: the square root of the scan rate vs. peak currents. (C) Plots: the logarithm of the scan rate vs. peak potential.

Fig. 3B exhibits a linear relationship between the square root of the scan rate and the peak current (linear regression equation as  $I_{pa} (\mu\text{A}) = 18.33v^{1/2} - 2.41$  ( $R^2 = 0.996$ )), indicating that mass transfer controls the electrode surface reaction [37, 38]. Moreover, the linear regression between the logarithm of the scan rate and the peak potentials can be presented as  $E_{pa} (\text{V}) = 0.09047 \log v + 0.2385$  ( $R^2 = 0.991$ ). Based on this relationship, the number of reaction-engaged electrons was obtained via Laviron's equation [39, 40]:

$$E_p = E^{\circ} + (2.303RT / \alpha nF) \log(RTk_o / \alpha nF) + (2.303RT / \alpha nF) \log v$$

where  $E^{\circ}$ ,  $R$ ,  $\alpha$ ,  $F$ , and  $k_o$  are, respectively, the formal redox potential, gas constant, electron transfer coefficient, Faraday's constant and standard heterogeneous rate constant of the reaction. When the slope of  $E_p$  vs.  $\log v$  is 0.09047, a value of 0.5495 can easily be obtained for  $\alpha n$ . Then,  $\alpha$  is computed as 0.7541 from the following formula:

$$E_{p/2} - E_p = 1.875(RT / \alpha F)$$

Hence, the total number of HY oxidation-engaged electrons is 2.

This work investigated the influence of pH on HY electro-determination. As the pH increases from 3 to 7, there is a gradual increase in peak current (Fig. 4A). The maximal peak current (126.6  $\mu$ A) was observed at pH 6. There is a decrease in peak current with a further pH increase. Hence a pH of 6 was used throughout the experiment. This study also investigated the effect of modifier quantity on the anodic peak current of HY. With the increase in modifier quantity (2 - 7  $\mu$ L), there is an obvious increasing tendency shown by the peak current (Fig. 4B). The current response decreases slightly as the modifier quantity is further increased, possibly due to the longer time for HY electrons to transport through the comparatively thicker RGO-ZnO film.

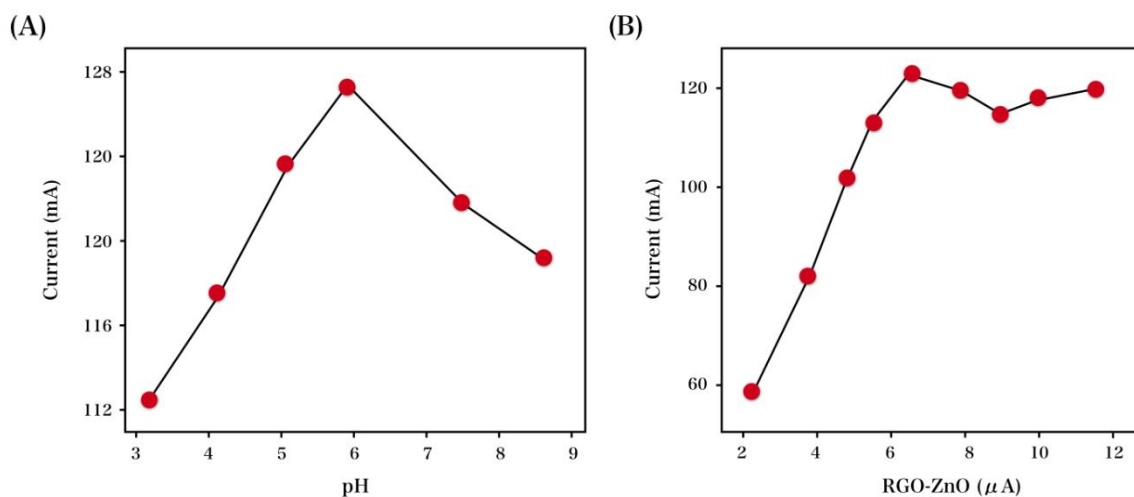


**Figure 4.** The plot of  $I_{pa}$  vs. (A) PBS pH (B) modifier quantity for the detection of HY.

The characteristic amperometric response that was obtained as soon as HY was successively added to RGO-ZnO modified GEC is displayed in Fig. 5. The RGO-ZnO modified GCE is observed to maintain a stable state within 5 s, indicating the fast response of the proposed biosensor to HY. The current response was found to be linearly related to the concentration of HY (1 - 800  $\mu$ M), with an LOD of 0.42  $\mu$ M (at a signal to noise ratio of 3). Herein, the linear regression equation was  $I (\mu A) = 0.10855 C(\mu M) + 16.9521$  ( $R^2 = 0.998$ ). As shown in Table 1, the performance of biosensor based on RGO-ZnO modified GEC for HY determination was comparable with other sensors.

Electrode	LDR ( $\mu$ M)	LOD ( $\mu$ M)	Reference
LC-ESI-MS	2-50	—	[41]

SEC/MALLS and sedimentation equilibrium	—	—	[42]
Polypyrrole-sulfonated graphene/hyaluronic acid-multiwalled carbon nanotubes	0.09-7	0.074	[43]
High-performance capillary electrophoresis RGO-ZnO/GCE	0.5-78	0.16	[44]
	1-800	0.42	This work

The effect of several physiological interferents was investigated to determine the selectivity of the as-prepared biosensor. The characteristic amperometric response of RGO-ZnO/GCE obtained as soon as HY was added, along with a range of possible interference groups such as acetylcholine (Ach), H<sub>2</sub>O<sub>2</sub>, glucose, dopamine (DA) and ascorbic acid (AA), is exhibited in Fig. 6. After DA, Ach, H<sub>2</sub>O<sub>2</sub>, glucose, and AA (1 mM) were added, the current response exhibited no pronounced variation, suggesting the desirable selectivity of the as-prepared biosensor to HY detection, even with a 2-fold excess of common interference groups.

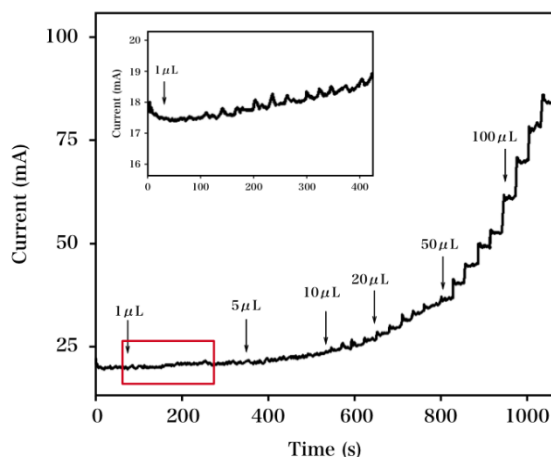


**Figure 5.** Amperometric response of the RGO-ZnO/GCE after consecutive additions of HY into the PBS. Inset indicates the magnification of current responses (1 - 10 μM).

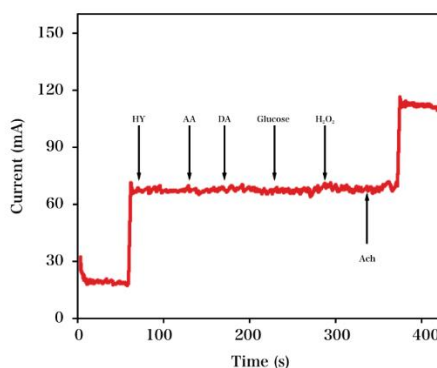


**Figure 6.** Amperometric current response of RGO-ZnO/GCE to the addition of HY (0.5 mM), AA (1 mM), DA (1 mM), glucose, H<sub>2</sub>O<sub>2</sub> and Ach.

HY (0.5 mM) was determined via six RGO-ZnO/GCEs to investigate the reproducibility of the as-prepared HY biosensor. A desirable relative standard deviation (RSD) of 3.1% was obtained, as indicated by the current responses. The successive 5000 s I-T test in HY (0.5 mM) was performed to investigate the stability of the as-prepared HY biosensor. As indicated by the results, there is a ca. 5% decrease in current response for the as-prepared biosensor. The proposed RGO-ZnO/GCE was stored in the refrigerator for 14 d to assess its long-term stability. After storage, the RGO-ZnO modified GCE exhibited over 93% of the primary activity, as indicated in the current response. Hence it can be concluded that the as-prepared HY biosensor is stable and reproducible. The concentration of HY in gecko extract specimens was measured to assess the practical behavior of the as-prepared HY biosensor. The concentration of HY was detected using the standard addition technique. Table 1 displayed the recovery rates of four experiments (97.70 - 102.64%). Hence the proposed HY biosensor has potential for application in HY concentration determination in real specimens.

**Table 1.** Determination of HY in gecko extract by RGO-ZnO modified GCE.

Sample	Content ( $\mu\text{M}$ )	Added ( $\mu\text{M}$ )	Found ( $\mu\text{M}$ )	Recovery (%)
1	13.51	10	22.97	97.70
2	10.25	20	31.05	102.64
3	27.55	50	76.84	99.08
4	26.32	100	127.60	101.01

#### 4. CONCLUSIONS

This work employed a facile one-pot hydrothermal approach to synthesize a novel RGO-ZnO nanocomposite. The selective HY detection was successfully realized by the proposed RGO-ZnO nanocomposite modified GCE. The fabricated HY biosensor exhibited a wide detection range, with low LOD and rapid response. This biosensor was stable and characteristic of anti-interference. Furthermore, the as-prepared biosensor has potential for application in the detection of HY in gecko extract samples.

#### References

1. A. Brichkina, T. Bertero, H. Loh, N. Nguyen, A. Emelyanov, S. Rigade, M. Ilie, P. Hofman, C. Gaggioli and D. Bulavin, *Genes & Development*, 30 (2016) 2623.
2. X. Tian, J. Azpurua, C. Hine, A. Vaidya, M. Myakishev-Rempel, J. Ablaeva, Z. Mao, E. Nevo, V. Gorbunova and A. Seluanov, *Nature*, 499 (2013) 346.
3. P. Auvinen, K. Rilla, R. Tumelius, M. Tammi, R. Sironen, Y. Soini, V. Kosma, A. Mannermaa, J. Viikari and R. Tammi, *Breast Cancer Research and Treatment*, 143 (2014) 277.
4. L. Bourguignon, G. Wong and M. Shiina, *Journal of Biological Chemistry*, 291 (2016) 10571.
5. A. Hallén, *Journal of Chromatography A*, 71 (1972) 83.
6. J. Scott, *Methods of Biochemical Analysis*, Volume 8, (1960) 145.
7. A. Linker, K. Meyer and P. Hoffman, *Journal of Biological Chemistry*, 235 (1960) 924.
8. Z. Dische, *Journal of Biological Chemistry*, 167 (1947) 189.

9. T. Hardingham and H. Muir, *Biochimica et Biophysica Acta (BBA)-General Subjects*, 279 (1972) 401.
10. V. Hascall and D. Heinegård, *Journal of Biological Chemistry*, 249 (1974) 4232.
11. T. Hardingham and P. Adams, *Biochemical Journal*, 159 (1976) 143.
12. A. Tengblad, *Biochemical Journal*, 185 (1980) 101.
13. U. Laurent and A. Tengblad, *Analytical Biochemistry*, 109 (1980) 386.
14. A. Engström-Laurent, U. Laurent, K. Lilja and T. Laurent, *Scandinavian Journal of Clinical and Laboratory Investigation*, 45 (1985) 497.
15. R. Brandt, E. Hedlöf, I. Åsman, A. Bucht and A. Tengblad, *Acta Oto-Laryngologica*, 104 (1987) 31.
16. B. Delpech, P. Bertrand and C. Maingonnat, *Analytical Biochemistry*, 149 (1985) 555.
17. R. Goldberg, *Analytical Biochemistry*, 174 (1988) 448.
18. P. Kongtawelert and P. Ghosh, *Analytical Biochemistry*, 178 (1989) 367.
19. A. Rössler, *Clinica Chimica Acta*, 270 (1998) 101.
20. X. Li, E. Thonar and W. Knudson, *Connective Tissue Research*, 19 (1989) 243.
21. K. Chichibu, T. Matsuura, S. Shichijo and M. Yokoyama, *Clinica Chimica Acta*, 181 (1989) 317.
22. L. Tang, Y. Wang, Y. Li, H. Feng, J. Lu and J. Li, *Adv Funct Mater*, 19 (2009) 2782.
23. L. Fu, A. Wang, Y. Zheng, W. Cai and Z. Fu, *Mater. Lett.*, 142 (2015) 119.
24. L. He, L. Fu and Y. Tang, *Catalysis Science & Technology*, 5 (2015) 1115.
25. L. Fu, Y. Zheng, Z. Wang, A. Wang, B. Deng and F. Peng, 10 (2015) 117.
26. F. Jiao, P. Qian, Y. Qin, Y. Xia, C. Deng and Z. Nie, *Talanta*, 147 (2016) 98.
27. H. Bai, S. Wang, P. Liu, C. Xiong, K. Zhang and Q. Cao, *Journal of Electroanalytical Chemistry*, 771 (2016) 29.
28. H. Li, K. Sheng, Z. Xie, L. Zou and B. Ye, *Journal of Electroanalytical Chemistry*, 776 (2016) 105.
29. P. Nayak, P.N. Santhosh and S. Ramaprabhu, *Graphene*, 1 (2013) 25.
30. L. Jiang, S. Gu, Y. Ding, F. Jiang and Z. Zhang, *Nanoscale*, 6 (2014) 207.
31. X. Zhang, D. Zhang, Y. Chen, X. Sun and Y. Ma, *Chinese Science Bulletin*, 57 (2012) 3045.
32. M. Ahmad, E. Ahmed, Z. Hong, N. Khalid, W. Ahmed and A. Elhissi, *J. Alloy. Compd.*, 577 (2013) 717.
33. M. Ahmad, E. Ahmed, Z. Hong, J. Xu, N. Khalid, A. Elhissi and W. Ahmed, *Appl. Surf. Sci.*, 274 (2013) 273.
34. C. Xu, X. Wang and J. Zhu, *J Phys Chem C*, 112 (2008) 19841.
35. D. Oukil, L. Benhaddad, R. Aitout, L. Makhlofi, F. Pillier and B. Saidani, *Sensors and Actuators B: Chemical*, 204 (2014) 203.
36. Y. Wei, M. Li, S. Jiao, Q. Huang, G. Wang and B. Fang, *Electrochimica Acta*, 52 (2006) 766.
37. Q. Guo and M. Li, *Int. J. Electrochem. Sci.*, 11 (2016) 7705.
38. D. Yadav, R. Gupta, V. Ganesan, P. Sonkar and P. Rastogi, *Journal of Applied Electrochemistry*, 46 (2016) 103.
39. E. Laviron, *J. Electroanal. Chem.*, 52 (1974) 355.
40. E. Laviron, *J. Electroanal. Chem.*, 101 (1979) 19.
41. M. Vigliano, A. Bianchera, R. Bettini and L. Elviri, *Chroma*, 76 (2013) 1761.
42. S. Hokputsa, K. Jumel, C. Alexander and S.E. Harding, *European Biophysics Journal*, 32 (2003) 450.
43. X. Xing, S. Liu, J. Yu, W. Lian and J. Huang, *Biosensors and Bioelectronics*, 31 (2012) 277.
44. S. Hayase, Y. Oda, S. Honda and K. Kakehi, *Journal of Chromatography A*, 768 (1997) 295.